Case Studies in Thermal Engineering 26 (2021) 101027

Contents lists available at ScienceDirect

Case Studies in Thermal Engineering

journal homepage: www.elsevier.com/locate/csite

Thermal properties of PEG/MOF-5 regularized nanoporous composite phase change materials: A molecular dynamics simulation

Pei Li [a], Daili Feng [a,b,*], Yanhui Feng [a,b,**], Jianrui Zhang [a], Yuying Yan [c], Xinxin Zhang [a,b]

[a] School of Energy and Environmental Engineering, University of Science and Technology Beijing, Beijing 100083, PR China
[b] Beijing Key Laboratory of Energy Conservation and Emission Reduction for Metallurgical Industry, School of Energy and Environmental Engineering, University of Science and Technology Beijing, Beijing, 100083, PR China
[c] Fluids & Thermal Engineering Research Group, Faculty of Engineering, University of Nottingham, Nottingham NG7 2RD, UK

HIGHLIGHTS

- The 3D full-through and regular structure of MOF-5 makes PEG a better stretchability therefore a low-dimensional effect.
- The scale effect of the melting point and latent heat of PEG nanowires in MOF-5 is weakened by the structure of MOF-5.
- The predicted latent heat of PEG/MOF composite material is as high as 78.4 kJ/kg with a mass filling rate of 50%.

GRAPHICAL ABSTRACT

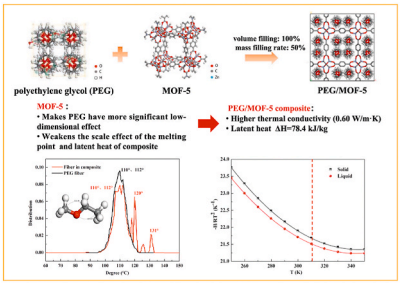

ARTICLE INFO

Keywords:
Polyethylene glycol
Metal organic frameworks
Shape stabilized phase change materials
Melting point

ABSTRACT

In this paper, a metal-organic framework MOF-5 loaded polyethylene glycol (PEG) nanowire was used to form composite phase change material PEG/MOF-5. The molecular dynamics method was used to simulate the thermal conductivity, melting point and latent heat by G-K function and pseudo-supercritical path method, respectively. The results show that the pores of MOF-5 promote the increase of the angle of the PEG main chain and the extension of the helical segment.

* Corresponding author. School of Energy and Environmental Engineering, University of Science and Technology Beijing, Beijing 100083, PR China.
** Corresponding author. School of Energy and Environmental Engineering, University of Science and Technology Beijing, Beijing 100083, PR China.
E-mail addresses: dlfeng@ustb.edu.cn (D. Feng), yhfeng@me.ustb.edu.cn (Y. Feng).

https://doi.org/10.1016/j.csite.2021.101027
Received 3 January 2021; Received in revised form 30 March 2021; Accepted 19 April 2021
Available online 1 May 2021

Latent heat
Thermal conductivity

Therefore, the thermal conductivity of the composite (0.60 W/m·K) is 17.6% and 100% higher than that of the PEG nanowire (0.51 W/m·K) and the skeleton (about 0.3 W/m·K), respectively. At the same time, MOF-5 can improve the crystallinity of the PEG to a certain extent. The predicted latent heat of PEG/MOF-5 composite material is as high as 78.4 kJ/kg with a mass filling rate of 50%. This paper explores the mechanism from a microscopic perspective in order to provide models and data for the thermal design of such materials.

Nomenclature

t	time, s
q	heat flow, W
V	volume, Å^3
G	Gibbs free energy, J/mol
H	enthalpy, J/mol
R	gas constant, J/mol·K
T	temperature, K
U^{vdw}	van der Waals force, eV
U^{elec}	Coulomb force, eV
m, n	positive integer power exponent
a_{ij}, b_{ij}	determined by potential well depth and width
k	thermal conductivity, W/m·K
c_v	heat capacity, J/m^3·K
$u_{p,g}$	phonon group velocity, m/s

Abbreviations

PEG	polyethylene glycol
PCMs	phase change materials
MOFs	metal organic frameworks
3D	three dimensional
ENG	expanded graphite
MD	molecular dynamics
PSCP	pseudo-supercritical path
WL	weakly interacting liquid
DWF	dense weak fluid
WC	weakly interacting crystal

Greek symbols

ε	sum of potential energy and momentum, eV
η	conversion factor
λ	coupling factor
λ_p	phonon mean free path, nm

Subscripts

ref	reference data
s-l	from the solid phase to liquid phase

1. Introduction

With the progressively serious situation of energy shortage and environmental pollution, the development of new energy resources and efficient energy storage systems has become the key to solve the energy crisis. Energy storage technology can effectively alleviate the imbalance in energy supply-consumption, improve energy efficiency, and protect the environment [1]. This technology can be used to store discontinuous, random energy in a suitable medium and release it when needed to achieve efficient use of energy [2,3].

Latent heat storage has been an important way for energy storage, characterized by small temperature fluctuation in energy storage process, large heat storage density and easy operation of energy storage system, and the key is phase change materials (PCMs) [4]. The development of new PCMs for energy storage through advanced thermal simulation technology and synthetic means is also a worldwide research hotspot in the field of energy and materials science in recent years [5]. Among them, the shaped composite phase change material has caused a lot of discussion in the field of energy storage because it can effectively solve a series of problems caused

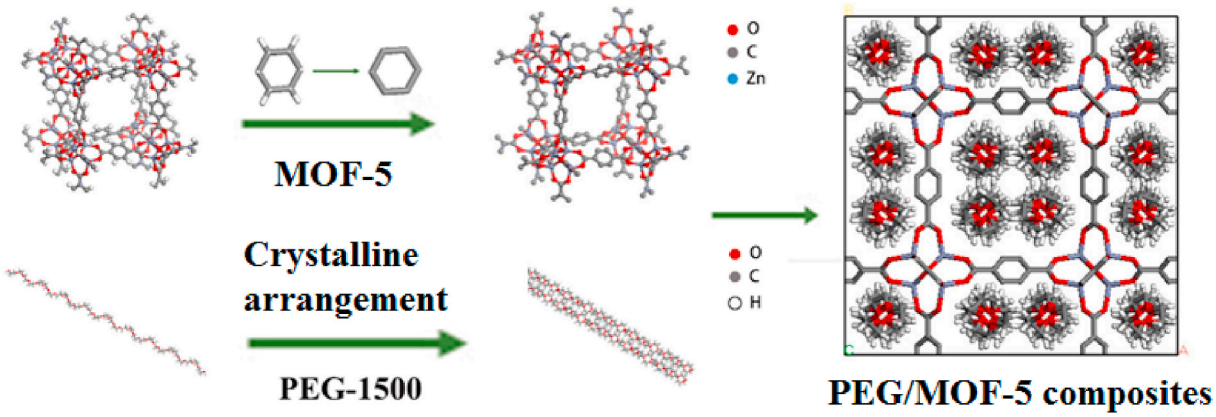

Fig. 1. Typical structure diagram of core, matrix and composite material.

by the easy leakage of amorphous PCMs. Porous-baseds are the most representative shaped PCMs [6], which utilize capillary effects, surface tension, chemical bonds of porous substrates, such as expanded graphite, diatomaceous earth, molecular sieves, Cr-MIL-101, etc. to effectively improve the reliability of phase change material storage in the substrate channel, so that the liquid leakage is less likely to occur when the material is phase-changed. Additionally, for the energy storage of the phase change material is caused by the low density and large specific surface area of the porous medium, energy storage density and heat transfer rate will be further improved.

However, due to the current imperfect preparation techniques and processes, most porous-based PCMs also have problems in sealing, heat conduction and stability. The composite mechanism between the core and shell material needs to be further explored. In addition, the correlation mechanism between the phase change thermal characteristics and mechanism and microstructure is not clear at this stage, which hinders the further optimization design of the shaped PCMs. Therefore, in order to obtain composite PCMs with outstanding thermal performance, in addition to continuously developing new combination of matrix and core material, thermal simulation technique for composite PCMs is also developed to guide the synthesis of novel composite PCMs [7].

Therefore, we propose to develop shaped PCMs based on metal organic frameworks (MOFs), and believe that based on their structural similarity and controllability, a thermal model of composite materials with certain versatility can be constructed to simulate and optimize the heat transfer performance of PCMs. MOFs [8] is a new type of three dimensional (3D) porous material that has developed rapidly in recent years, consisting of metal clusters, such as Zn, Al, Cr, etc. and organic ligands, such as terephthalic acid, 1, 4-benzene, the 1,3,5-tricarboxylate, etc. They are controllable in pore size, shape and dimension, and the preparation method is simple and low-cost. As an emerging synthetic material, it is widely used in gas storage, adsorption and catalysis fields. MOF-5 has a full-through and regular pore structure, large specific surface area (2900 m^2/g) [9] and good thermal stability, which remains stable after being heated to 300 °C. As for a phase change material, polyethylene glycol (PEG) has become one of the most popular medium-low temperature organic PCMs, which has the advantages of non-reactive, no phase separation and nontoxic [10]. Compared with macroscopic polymers, the confined polymers would exhibit unique properties in the motion of molecular and phase transition. However, studies on the thermal properties of MOFs are very limited, mainly focusing on heat capacity testing, and thermal conductivity has rarely been reported. In terms of heat capacity, in 2014, Yang et al. [11] heated the sample of MOF-5 powder at a heating rate of 5 °C/min at 220–370 K, and measured the heat capacity of the MOF-5 powder at 300 K is 0.72 J/g·K. During the process of increasing the sample temperature from 220 K to 340 K, the heat capacity increased from 0.6 J/g·K to 0.8 J/g·K, an increase of 33%. In 2012, Liu et al. [12] experimentally studied the effect of expanded graphite (ENG) additives on the heat capacity of MOF-5. They measured the heat capacity of the sample before and after adding the ENG at 26, 35, 45, 55 and 65 °C by differential scanning calorimetry, and found that the heat capacity shows an upward trend with the increases of temperature. For samples with a constant density, the heat capacity increases as the ENG content increases. As for thermal conductivity, in 2007, Huang et al. [13] tested the thermal conductivity of MOF-5 crystal sample at 6–300 K, and obtained the highest and lowest thermal conductivity of the sample is 0.37 W/m·K (20 K) and 0.22 W/m·K (100 K), respectively. In the same year, Huang et al. [14] studied the heat transfer characteristic of MOF-5 using equilibrium molecular dynamics (MD) simulation, which agrees well with the experimental values.

Composite PCMs based on MOFs and their thermal properties have not been reported so far. In this paper, a composite phase change material PEG/MOF-5 with MOF-5 loaded PEG nanowires was proposed, and its phase transition thermal characteristics, including melting point, latent heat and thermal conductivity, were predicted by MD simulation. The model and simulation method were validated by comparing the simulated values of PEG bulk with experimental data. The simulations were carried out on porous matrix MOF and PEG nanowires respectively, in order to compare them with their composites, focusing on the effect of matrix packaging on the phase transition of the core material. Breaking through the traditional “try and error” method, which is blindness and unpredictability, this work attempts to predict and explore the thermal characteristics and mechanism of composite PCMs based on MOF-5, in order to provide theoretical models and data for the thermal design of such PCMs.

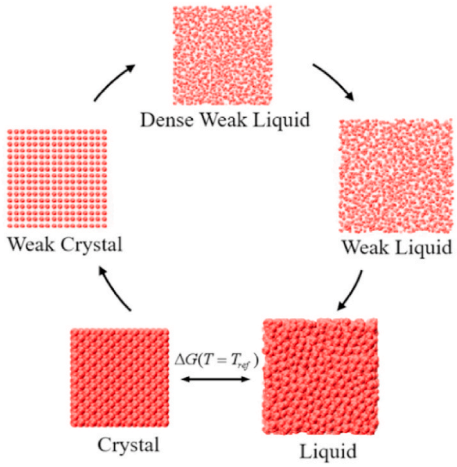

Fig. 2. PSCP path diagram. (Revised from [19], copyright 2012, AIP publishing).

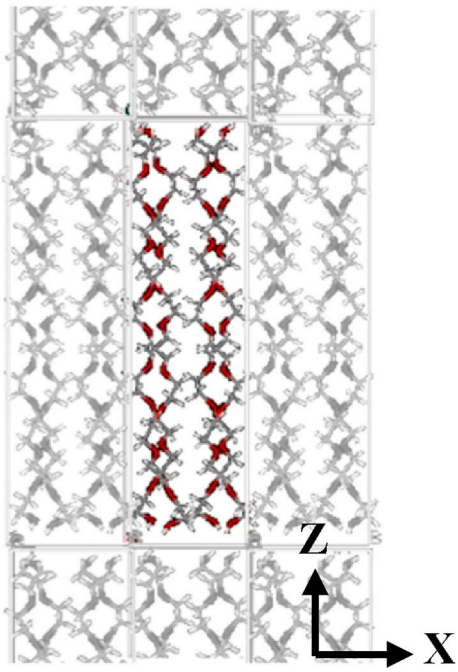

Fig. 3. Structural model of PEG-1500 crystal bulk (Red: O; Gray: C; White: H). (For interpretation of the references to colour in this figure legend, the reader is referred to the Web version of this article.)

2. Model and simulation method details

2.1. Nano-structural model construction

The models of MOF-5 and PEG were constructed by Material Studio software according to the structural parameters from Cambridge Crystallographic Data Center (CCDC). Fig. 1 shows the structural modeling process of PEG/MOF-5 composite. The matrix material MOF-5 has a 3D through-hole structure, which contains two kinds of pores with different sizes, and the pore diameters are 0.97 nm and 1.1 nm, respectively. The chemical formula of matrix material is $8[Zn_4O(BDC_3)]$ and its lattice constant is 25.85 Å. The simulated XRD of MOF-5 was compared with that of the experiment [15] (Supporting Information Fig. S1). It can be seen that the main peak positions of the simulated XRD are consistent with that of the experiment [15], which verifies the rationality and correctness of the model in this paper. During the simulation, the C–H group on the benzene ring was regarded as a rigid body structure, that is, the mass of the H atom was added to the adjacent C atom. The core material PEG is polymerized by $–OC_2H_4-$ monomer, and the chain segment of the crystal structure exists in a spiral stretch form. This paper simulated a PEG nanowire with 34 repeating monomers. The

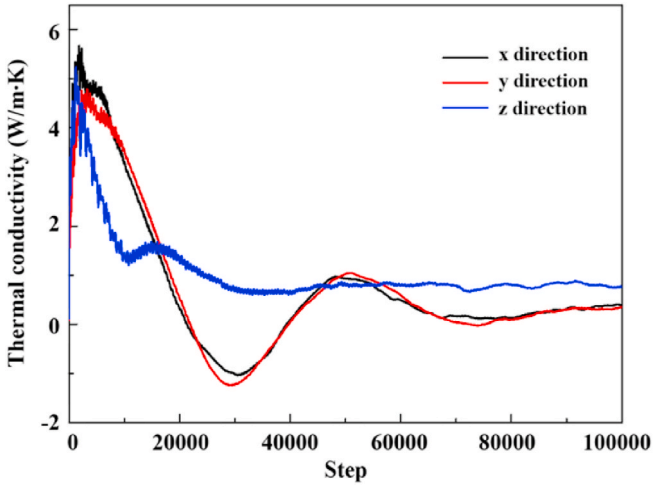

Fig. 4. Thermal conductivity of PEG-1500 bulk.

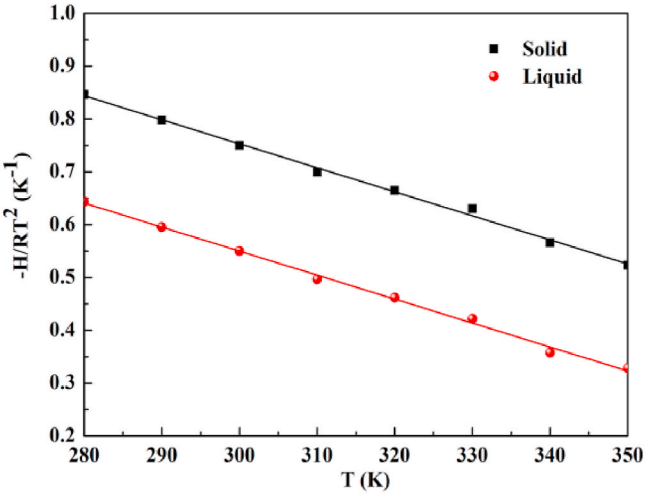

Fig. 5. $-H/RT^2$ curves of solid and liquid phases of PEG1500 bulk.

length of the segment is 9 nm and the molecular mass of PEG nanowire is 1500. The composite material consists of PEG nanowires and MOF-5. The PEG nanowires were uniformly and regularly filled in the MOF-5 channel. The volume filling rate is 100%, and the mass filling rate is 50%. After the energy minimization process, the MD simulation was performed using open-source LAMMPS software on TianHe-1(A) at National Supercomputer Center in Tianjin. The CHARMM32 [16] force field was used to describe the interatomic force within the PEG. The potential function of MOF-5 was taken from the literature [14], and the weak force between PEG and MOF-5 was expressed by the L-J [17] potential according to the Lorentz-Berthelot mixing rule. Atom types and potential parameters of PEG and MOF-5 were shown in the Supporting Information Figs. S2–S3, Tables S1–S2, respectively.

2.2. Phase change characteristics calculation

The equilibrium MD method was performed to calculate the thermal conductivity of the material. According to the law of relaxation, if the temperature gradient is meaningful, the heat flow changes satisfy the following formula when the steady state is not reached:

$$\frac{d\vec{q_s}}{dt} = \frac{\vec{q} - \vec{q_s}}{T} \tag{1}$$

where t is phonon relaxation time (s), q refers to the steady state heat flow (W), q_s is the heat flow (W) at the non-steady state. In the equilibrium state, since there is no temperature gradient, thus q = 0. And

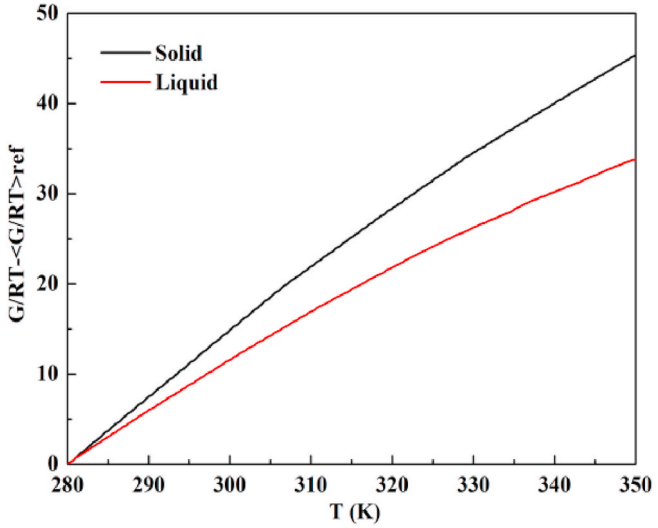

Fig. 6. $G/RT-<G/RT>_{ref}$ curves with the change of temperature.

$$\overrightarrow{q_s}=\frac{1}{V}\left[\sum_i \overrightarrow{v_i}\varepsilon_i+\sum_{i<j}\overrightarrow{x}_{ij}\left(\overrightarrow{F_{ij}}\cdot\overrightarrow{v_j}\right)\right] \tag{2}$$

where ε is the sum of potential energy and momentum (eV). According to the G-K formula, thermal conductivity can be obtained by the calculation and integration of auto-correlation of the heat flow.

$$k=\frac{V}{3k_B T^2}\int_0^\infty \langle \overrightarrow{q_s}(t)\cdot\overrightarrow{q_s}(0)\rangle dt \tag{3}$$

Where V is the volume of the simulated system ($Å^3$). The time step was 0.5 fs. Firstly, the system was relaxed under the NVT ensemble, and then the thermodynamic information of the system was calculated under the NVE ensemble. The total simulation duration was 5 ns.

The pseudo-supercritical path method (PSCP) was performed to simulate the phase transition characteristics of materials. The detailed theory of the method has been described in literature [18,19]. The key basis for the determination of the melting point by the PSCP method is that the Gibbs free energy of the crystal phase and liquid phase is equal at the melting point temperature, and the difference in Gibbs free energy can be calculated according to the Gibbs-Helmholtz equation:

$$\frac{G}{RT}-\left(\frac{G}{RT}\right)_{ref}=\int_{T_{ref}}^{T}-\frac{H}{RT^2}dT \tag{4}$$

Where G is the Gibbs free energy (J/mol), H is the enthalpy (J/mol), R is the gas constant (J/mol·K), T is temperature (K). The simulation solved the equation consisting of two major parts: Firstly, the enthalpy values of solid phase and liquid phase were calculated under the NPT ensemble to obtain a curve $-\frac{H}{RT^2}$ about the temperature. Secondly, at a certain reference temperature (T_{ref}), the Gibbs free energy change of solid phase and liquid phase was calculated, that is, obtained by thermodynamic integration:

$$\Delta\left(\frac{G}{RT}\right)_{ref}=\frac{\sum\left(\int_0^1\left\langle\frac{\partial U}{\partial\lambda}\right\rangle_\lambda d\lambda\right)}{RT}+\frac{P\Delta V_{s-l}}{RT} \tag{5}$$

The Gibbs free energy difference between the crystal and liquid phases is only related to the initial state and has nothing to do with the path. The method assumes that the crystal phase and the liquid phase are virtually connected by weakly interacting liquid (WL), dense weak fluid (DWF) and the weakly interacting crystal (WC), as shown in Fig. 2. The WC state can be obtained by weakening the long-range force and adding the tethering potential function. The new long-range force expression is:

$$U(\lambda)=[1-\lambda(1-\eta)]^m U^{vdw}+[1-\lambda(1-\eta)]^n U^{elec}-\lambda\sum_i\sum_j a_{ij}\exp\left(-b_{ij}r_{ij}^2\right) \tag{6}$$

Where, U^{vdw} and U^{elec} are the van der Waals force and Coulomb force in the potential function, respectively, η is conversion factor between 0 and 1, m and n are positive integer power exponents, λ is coupling factors between 0 and 1. The values of the parameters a_{ij}

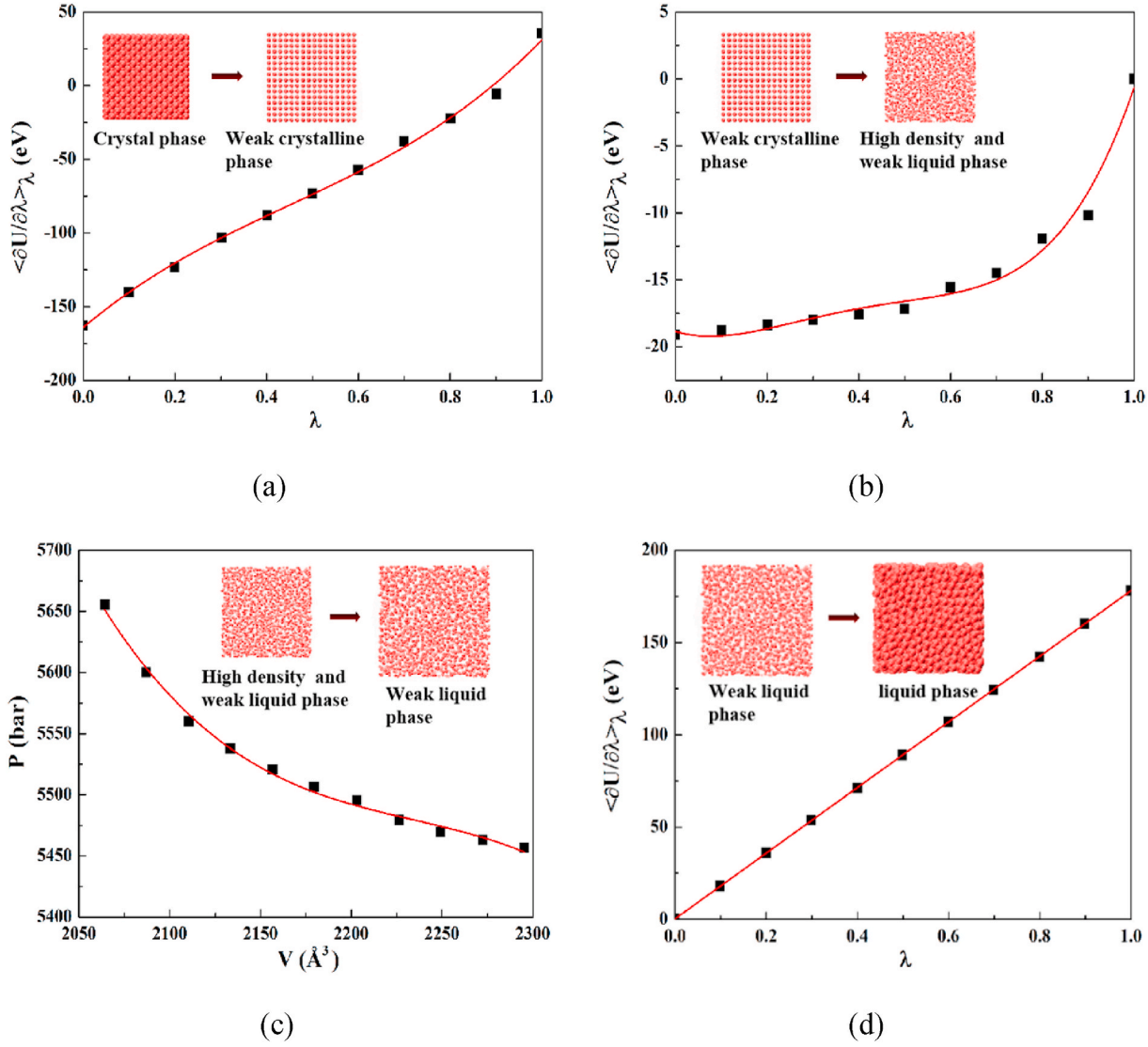

Fig. 7. Curves of the thermodynamic integral.

and b_{ij} were determined by the width and depth of the potential well of the material.

DWF can be obtained by eliminating the tethering force in WC, and then the volume of the DWF was gradually expanded to the liquid volume of the material, so that WL can be obtained. Finally, the long-range force of the system was restored to obtain a stable liquid phase.

The free energy of the crystal phase and liquid phase were carried out under the NPT ensemble, the temperature range was 280–350 K, and the total simulation time was 2 ns. The data was statistically analyzed in the last 1 ns. The simulation process along the PSCP was performed under the NVT ensemble, and λ gradually increased in steps of 0.1 between 0 and 1, and the total simulation time was 80 ns.

3. Results and discussions

3.1. Verification of models and methods

Due to the limited thermal research on the crystalline PEG nanowires at present, the thermal properties of the PEG bulk, including the thermal conductivity, melting point and latent heat, as shown in Figs. 3–8, were simulated first and compared with the tested data to verify the reliability of the models.

Fig. 3 shows the structural model of PEG-1500 bulk, which has periodic boundary conditions in the directions of X, Y and Z. The direction of Z is the same as the direction of crystal segment. In order to eliminate the influence of the size effect of the analog box, the

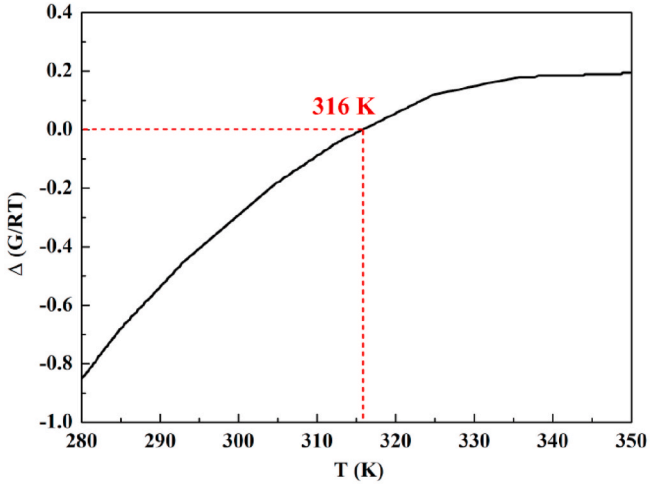

Fig. 8. Curve of Gibbs free energy difference of solid-liquid phase of PEG bulk with the change of temperature.

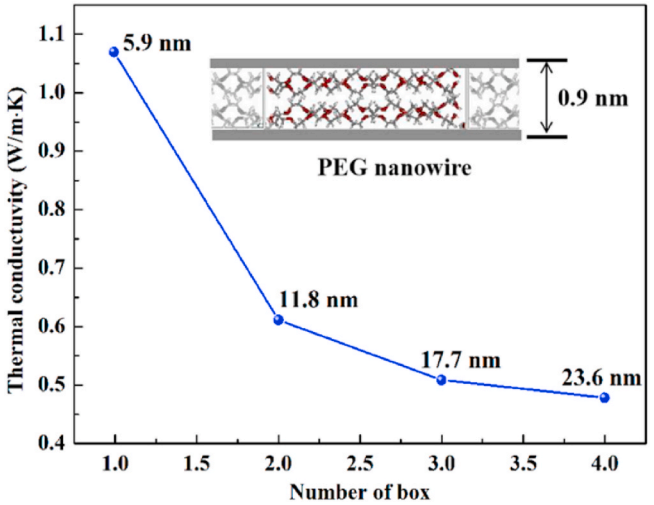

Fig. 9. Size effect of simulation box on the thermal conductivity of PEG nanowire.

simulation box was selected to calculate the thermal conductivity convergence curve under 200 K. As shown in Fig. 4, it can be seen that the thermal conductivity in the three directions converges to 0.28, 0.25, 0.70 W/m·K, respectively, and the average thermal conductivity is 0.41 W/m·K, showing the same order of magnitude as the experimental data [20] (0.29 W/m·K), but larger than that of the experiment. This is because the actual bulk contains both crystalline and amorphous states, while the simulated object is completely crystalline. The atomic arrangement is long-range and orderly, resulting in a small probability of phonon collision and a large average free path. In addition, the thermal conductivity of PEG exhibits a strong anisotropy with an anisotropy index of $2K_z/(K_x + K_y) = 2.64$. This is due to the fact that the heat is conducted along the covalent bond in the direction of the chain (z direction), while is conducted through molecular collision in the direction of the vertical segment (x, y direction), thus the thermal conductivity in the direction of the segment is significantly larger than that of the other two directions.

Considering that the PSCP method is not affected by the size effect of the analog box [21], the simulation used a minimum simulation box containing 5280 atoms to reduce the amount of calculation. Fig. 5 shows the curves of $-H/RT^2$ with the change of temperature in solid and liquid phases. After being fitted to a quadratic curve, the relative free energy was obtained by integrating according to formula (4), as shown in Fig. 6. Then a thermodynamic integration cycle was carried out at 280 K (reference temperature) in order to get a Gibbs free energy difference, each part is fitted by a polynomial, as shown in Fig. 7. The Gibbs free energy difference of PEG at 280 K can be obtained by adding the change of free energy of each part. Substituting the value into formula (4) can obtain the curve of $\Delta(G/RT)$ with the change of temperature, as shown in Fig. 8. The melting point of PEG-1500 is determined to be 316 K by the intersection of the curve and the 0 line, and the error from the experimental value [22] (318 K) is only 0.6%. At the same time, the phase transition enthalpy of PEG-1500 can be determined by the enthalpy difference of solid-liquid phase at 316 K. According to the fitting curve in Fig. 5, the phase transition enthalpy of PEG-1500 is 167 kJ/kg, which was in good agreement with the experimental

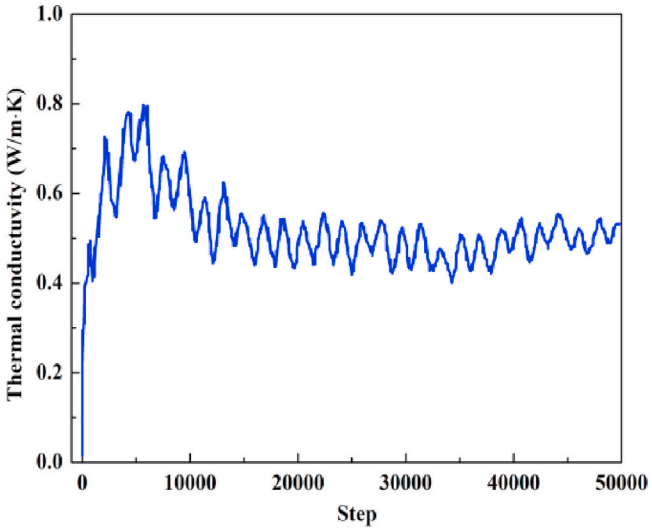

Fig. 10. Thermal conductivity of PEG-1500 nanowire segment.

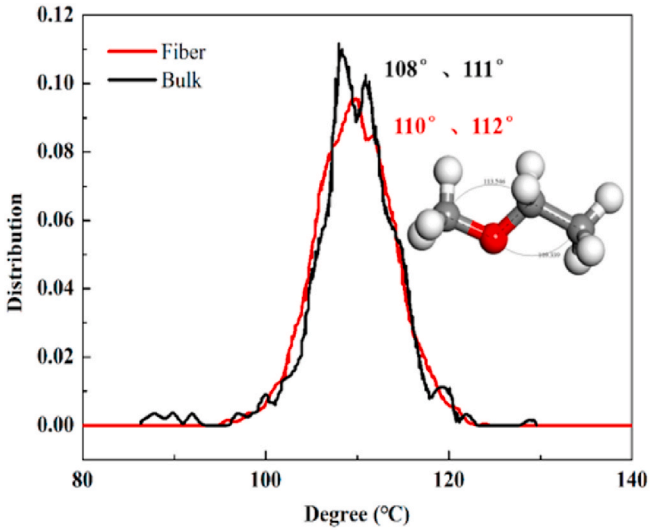

Fig. 11. The angle distribution of atoms on PEG-1500 main chain.

values [23] (170 kJ/kg).

3.2. *Thermal properties of polyethylene glycol nanowires*

Considering that the main form of PEG in the pores of MOF-5 is nanowires, the thermal properties of pure PEG nanowires were simulated first.

Fig. 9 (insert) shows the structural model of PEG nanowires. The direction along the chain length is a periodic boundary condition, while the direction perpendicular to the chain length is a free boundary condition. Since the substrate MOF-5 usually contains two kinds of pores with pore diameters of 0.97 nm and 1.1 nm, respectively, this section simulated PEG nanowires having a cross-sectional side length of 0.9 nm.

In order to eliminate the influence of the size effect of simulated box on the heat conduction, the simulations of thermal conductivity with different size of simulation boxes ($1 \times 1 \times 1$,$1 \times 1 \times 2$,$1 \times 1 \times 3$ and $1 \times 1 \times 4$) were carried out respectively. As shown in Fig. 9, when there are three analog boxes in the length direction, the error is less than 5% as the number of boxes increases. Therefore, the thermal conductivity of the nanowires was calculated by using the $1 \times 1 \times 3$ simulation box.

Fig. 10 exhibits the convergence of the thermal conductivity in z-direction of PEG-1500 nanowire with an infinitely length at 200 K. The thermal conductivity converges to 0.51 W/m·K, which is significantly smaller than that of the bulk (0.70 W/m·K). Henry et al. [24]

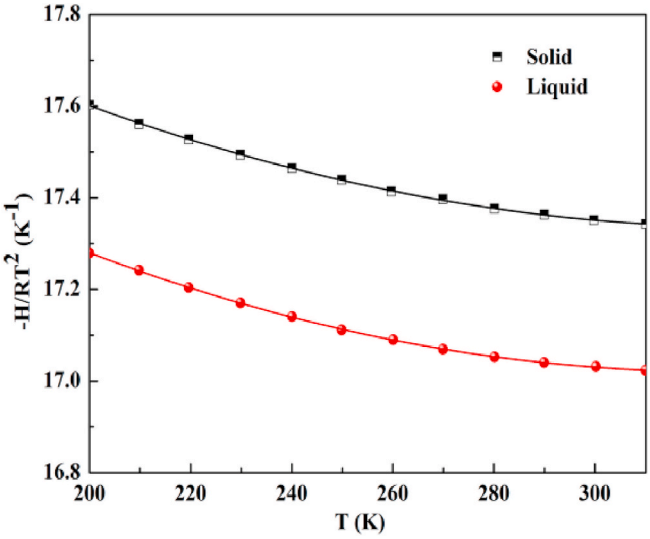

Fig. 12. *-H/RT^2* curves of solid and liquid phase of PEG nanowire.

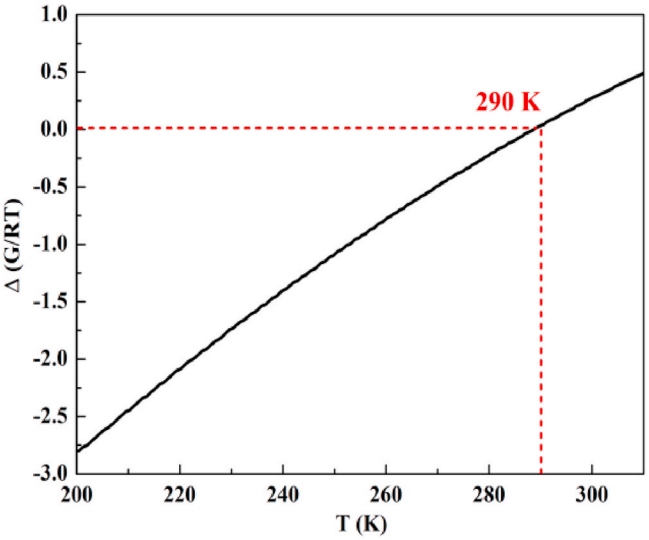

Fig. 13. Curve of Gibbs free energy of PEG nanowire with the change of temperature.

pointed out that the increase in the angle of the polymer backbone (the degree of stretching) facilitates heat transfer. Moreover, the thermal conductivity reduces as the scale decreases due to the scale effect of the material at the nanoscale [25]. By comparing the angles of the backbone chains of the PEG segments between the nanowires and bulk (Fig. 11), it can be seen that the nanowires did not exhibit significant stretching. Therefore, the thermal conductivity of PEG nanowires is mainly affected by the scale effect, which is significantly reduced.

According to the PSCP method, the enthalpy of solid and liquid phases of PEG nanowires at different temperatures as well as the Gibbs free energy difference between solid and liquid phases at 200 K were calculated. Substituting the value into formula (4) can obtain the curve of Δ*(G/RT)* with the change of temperature, as shown in Fig. 12 and Fig. 13. It is known that the melting point of the PEG-1500 nanowire is 290 K and the latent heat is 149 kJ/kg. There is a slight decrease compared with the value of the macro material.

3.3. Thermal properties of PEG/MOF-5 composite phase change material

According to the calculation results of the PEG nanowires above, by simulating the thermal characteristics of PEG/MOF-5, the influence of the MOF-5 substrate on the phase change thermal properties of the PEG filler can be revealed. It was assumed that PEG was filled in the pores of MOF-5 in crystalline form.

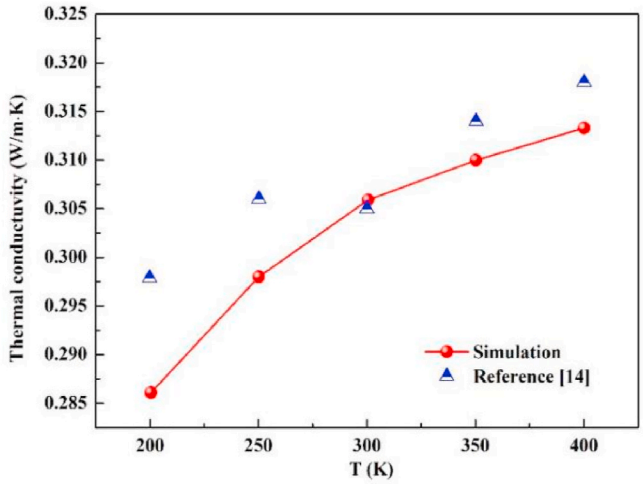

Fig. 14. Simulation results of MOF-5 thermal conductivity [14].

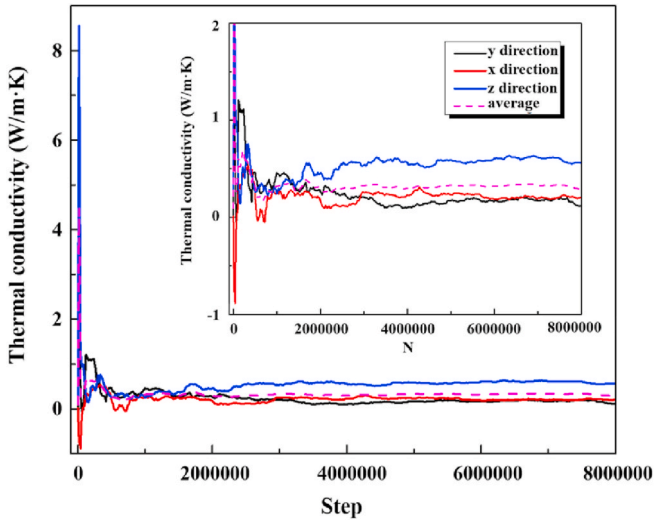

Fig. 15. Thermal conductivity of PEG/MOF-5 composites.

As a substrate for shaped PCMs, MOF-5 does not undergo phase transformation, but participates in the heat conduction of composite phase change material. Therefore, to reveal the effect of MOF-5 on the heat transfer of PEG fillers, the thermal conductivity of MOF-5 was clarified first and compared with the MD simulation value of Huang et al. [14] (Fig. 14). The results are similar. The average thermal conductivity of MOF-5 with an average pore diameter of about 1 nm at 300 K is about 0.3 W/m·K, which is lower than the thermal conductivity of expanded graphite, silica, etc., but higher than that of the polymers and molecular sieve porous materials. According to the kinetic theory:$k = c_v u_{p,g} \lambda_p / 3$, the thermal conductivity k is determined by the heat capacity c_v (J/m^3·K), the phonon group velocity $u_{p,g}(m/s)$, and the phonon mean free path λ_p(nm). The 3D full-through and regular structure of MOF-5 leads to a low atomic density and thus a small heat capacity. Moreover, MOF-5 is consist of splicing organic segments formed by phenylene groups and metal clusters formed by zinc and oxygen atoms. The freedom degree of the phenylene groups and the mass of the metal clusters are both large, resulting in a very low phonon group velocity. At the same time, the cluster structure also inhibits the motion of long-range phonons, resulting in a lower mean free path of the phonon, thus MOF-5 has a lower thermal conductivity. In addition, the thermal conductivity of MOF-5 shows a weaker temperature dependence. At the temperature of 200–400 K, the thermal conductivity increases by only 9.5% with the rises of temperature, which is close to the weak temperature dependence of amorphous phase.

When MOF-5 was combined with PEG nanowires with a side length of 0.9 nm, the convergence curves of the thermal conductivity were shown in Fig. 15. It can be seen that at 200 K, the thermal conductivity in the three directions of x, y, and z converges to 0.17, 0.20, and 0.60 W/m·K, respectively. The anisotropy index is 3.24, and the average thermal conductivity is 0.32 W/m·K, which is lower than that of the PEG crystalline bulk (0.41 W/m·K). But excitingly, the thermal conductivity of PEG/MOF-5 along the core segment direction (z direction) is greater than that of the PEG nanowire and MOF-5 framework. Considering the increase of anisotropy index of

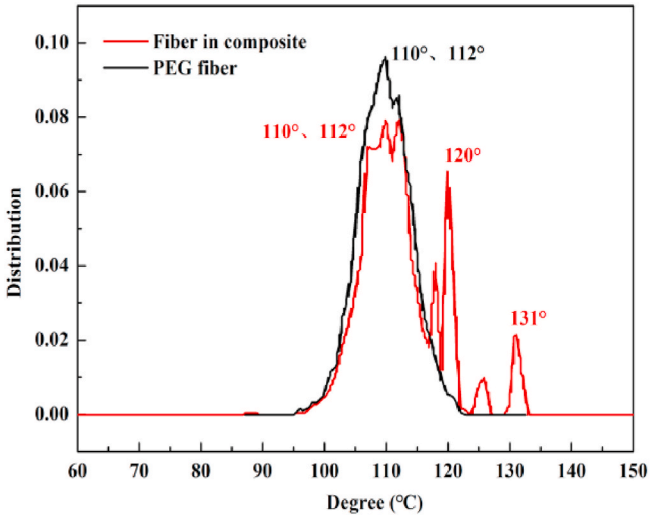

Fig. 16. Angle distribution curves of main chain atoms before and after PEG nanowires filling.

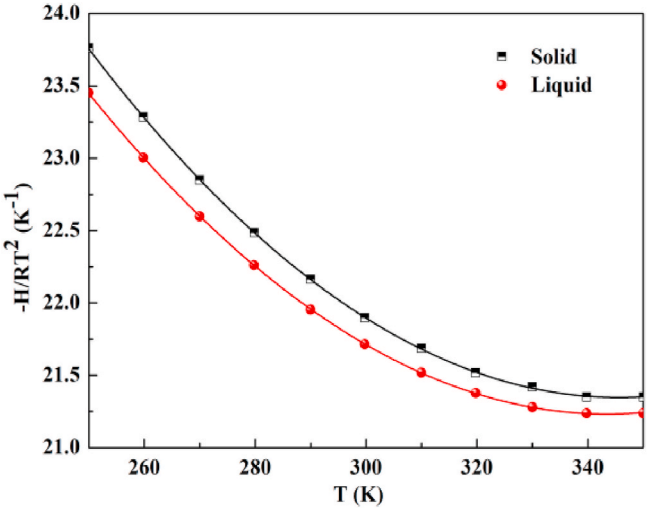

Fig. 17. $-H/RT^2$ Curves of solid and liquid phases of PEG nanowires in the composites.

the composite material's thermal conductivity, we believe that this special phenomenon is due to the obvious extension of the PEG segment in MOF-5 channels, that is, the angle of the main chain atom is significantly increased, as shown in Fig. 16. This is due to the fact that the segment of the polymer PEG is in a highly regular and stable structure, and the interatomic interaction forces are more directional with respect to the macromaterial [26]. That is to say, the PEG nanowires filled into the pores of MOF-5 have a more significant low-dimensional effect, so the thermal conductivity of the composite is greater than that of the pure PEG nanowires, and the thermal conductivity in the z-direction of the composite material is greater than that of the two constituent materials.

Since the substrate MOF-5 does not participate in the phase transition, MOF-5 was regarded as a rigid body structure when the phase transition property of the composite was simulated. Only the interatomic force of PEG and the interaction force between MOF-5 and PEG were considered. The phase transition characteristics of the composite were calculated according to the PSCP method. As shown in Figs. 17 and 18 and Table 1, the melting point of the composite material is higher than that of the PEG nanowire, which is because the 3D full-through structure of the substrate weakens the scale effect of PEG filler. The latent heat of PEG/MOF-5 (78.4 kJ/kg) is equivalent to the product of the latent heat value of the pure PEG nanowire (149 kJ/kg) and the mass ratio of the nanowire in the composite (50%) (74.5 kJ/kg), even there is an increase; that is, the crystallization of PEG in the 3D full-through and regular pore structure of MOF-5 is not limited. This phenomenon has also been discovered by other scholars [27], but its internal mechanism needs to be further studied.

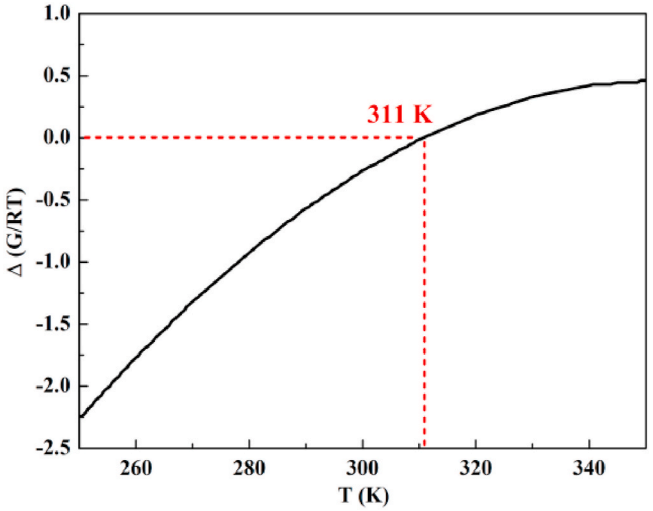

Fig. 18. The variation of Gibbs free energy of PEG nanowires with temperature in the composites.

Table 1
Simulation values of phase change thermal properties of substrate, core material and the composite.

material	thermal conductivity in the chain direction(200 K, W/m·K)	melting point(K)	latent heat(kJ/kg)
PEG-1500 bulk	0.70	316	167.0
PEG-1500 nanowires	0.51	290	149.0
MOF-5	0.286(Isotropy)	–	–
PEG/MOF-5 composites	0.60	311	78.4

4. Conclusion

In this paper, a composite phase change material, PEG/MOF-5, formed by metal-organic framework MOF-5 loaded polyethylene glycol PEG nanowires was proposed, and the phase change thermal properties was simulated by MD method. The thermal conductivity was calculated by G-K function, and the melting point and latent heat were calculated by PSCP method. Our predictions show that MOF-5 is a viable porous matrix for encapsulating PCMs, which can effectively facilitate the heat transfer of PCMs. The main conclusions of the full text are as follows:

(1) The thermal conductivity, melting point and latent heat of the PEG bulk agree well with the tested values, which verifies the reliability of the model and the simulation method. The heat is conducted along the covalent bond in the direction of the chain, while it is conducted through molecular collision in the direction of the vertical segment. Therefore, the thermal conductivity of the PEG bulk segment in z direction is significantly larger than that of the other two directions, showing strong anisotropy.
(2) The segment of the pure PEG nanowires has no obvious extension compared with the macroscopic crystalline state, and its thermal conductivity in the length direction of the segment is 0.51 W/m·K, which is smaller than that of the PEG bulk material. However, the scale effect of the melting point and latent heat of the nanowires is not obvious, and there is only a small decrease relative to the bulk.
(3) The filled nanowires are obviously extended in the pores of MOF-5, and the angle of the main chain atoms of the segment is increased, which is favorable for heat conduction, and compensates for the defects of low thermal conductivity of the substrate MOF-5 (about 0.3 W/m·K), so that the composite material exhibits good heat transfer characteristics. At 200 K, the thermal conductivity of the composite segment is 0.60 W/m·K, which is larger than pure nanowires (0.51 W/m·K) and skeleton, increasing by 17.6% and 100%, respectively. The anisotropy of the thermal conductivity of the composite is mainly derived from the core material.
(4) The composite phase change material has good heat storage characteristics. The predicted latent heat is as high as 78.4 kJ/kg with a mass filling rate of 50%, which is greater than the theoretical value of 74.5 kJ/kg. The reason and internal mechanism need to be further studied and determined.

CRediT authorship contribution statement

Pei Li: Software, Methodology, Visualization, Writing – original draft. **Daili Feng:** Conceptualization, Methodology, Project administration, Funding acquisition, Writing-Reviewing and Editing. **Yanhui Feng:** Conceptualization, Methodology, Project

administration, Funding acquisition. **Jianrui Zhang:** Software, Methodology, Visualization. **Yuying Yan:** Methodology, Supervision. **Xinxin Zhang:** Supervision.

Declaration of competing interest

The authors declare that they have no known competing financial interests or personal relationships that could have appeared to influence the work reported in this paper.

Acknowledgments

Thanks for the support provided by the Beijing Natural Science Foundation (No.3192022), National Natural Science Foundation of China (No.51876007) and Fundamental Funds for the Central Universities (FRF-BD-20-09A).

Appendix A. Supplementary data

Supplementary data to this article can be found online at https://doi.org/10.1016/j.csite.2021.101027.

References

[1] M. Yu, S.H. Hong, Supply–demand balancing for power management in smart grid: a Stackelberg game approach, Appl. Energy 164 (2016) 702–710, https://doi.org/10.1016/j.apenergy.2015.12.039.
[2] F. Agyenim, N. Hewitt, P. Eames, et al., A review of materials, heat transfer and phase change problem formulation for latent heat thermal energy storage systems (LHTESS), Renew. Sustain. Energy Rev. 14 (2010) 615–628, https://doi.org/10.1016/j.rser.2009.10.015.
[3] H. Zhang, J. Baeyens, G. Caceres, et al., Thermal energy storage: recent developments and practical aspects, Prog. Energy Combust. Sci. 53 (2016) 1–40, https://doi.org/10.1016/j.pecs.2015.10.003.
[4] D.L. Feng, Y.H. Feng, L. Qiu, et al., Review on nanoporous composite phase change materials: fabrication, characterization, enhancement and molecular simulation, Renew. Sustain. Energy Rev. 109 (2019) 578–605, https://doi.org/10.1016/j.rser.2019.04.041.
[5] D. Lencer, M. Saling, B. Grabowski, et al., A map for phase-change materials[J], Nat. Mater. 7 (2008) 972–977, https://doi.org/10.1038/nmat2330.
[6] G. Aad, T. Abajyan, B. Abbott, et al., Measurements of top quark pair relative differential cross-sections with ATLAS in pp collisions at\ sqrt {s}= 7\ mbox {TeV}, European Physical Journal C 73 (2013) 1–28, https://doi.org/10.1140/epjc/s10052-012-2261-1.
[7] T. Nomura, N. Okinaka, T. Akiyama, Impregnation of porous material with phase change material for thermal energy storage, Mater. Chem. Phys. 115 (2009) 846–850, https://doi.org/10.1016/j.matchemphys.2009.02.045.
[8] L.F. Song, J. Zhang, L.X. Sun, et al., Mesoporous metal–organic frameworks: design and applications, Energy Environ. Sci. 5 (2012) 7508–7520, https://doi.org/10.1039/c2ee03517k.
[9] H. Li, M. Eddaoudi, M. O'Keeffe, et al., Design and synthesis of an exceptionally stable and highly porous metal-organic framework, Nature 402 (6759) (1999) 276, https://doi.org/10.1038/46248.
[10] D.L. Feng, Y.Y. Zang, P. Li, et al., Polyethylene glycol phase change material embedded in a hierarchical porous carbon with superior thermal storage capacity and excellent stability, Compos. Sci. Technol. 210 (2021) 108832, https://doi.org/10.1016/j.compscitech.2021.108832.
[11] Y. Ming, J. Purewal, D.A. Liu, et al., Thermophysical properties of MOF-5 powders, Microporous Mesoporous Mater. 185 (2014) 235–244, https://doi.org/10.1016/j.micromeso.2013.11.015.
[12] D. Liu, J.J. Purewal, J. Yang, et al., MOF-5 composites exhibiting improved thermal conductivity, Int. J. Hydrogen Energy 37 (2012) 6109–6117, https://doi.org/10.1016/j.ijhydene.2011.12.129.
[13] B.L. Huang, Z. Ni, A. Millward, et al., Thermal conductivity of a metal-organic framework (MOF-5): Part II. Measurement, Int. J. Heat Mass Tran. 50 (2007) 405–411, https://doi.org/10.1016/j.ijheatmasstransfer.2006.10.001.
[14] B.L. Huang, A.J. H McGaughey, M. Kaviany, Thermal conductivity of metal-organic framework 5 (MOF-5): Part I. Molecular dynamics simulations, Int. J. Heat Mass Tran. 50 (2007) 393–404, https://doi.org/10.1016/j.ijheatmasstransfer.2006.10.002.
[15] C.M. Wu, M. Rathi, S.P. Ahrenkiel, et al., Facile synthesis of MOF-5 confined in SBA-15 hybrid material with enhanced hydrostability, Chem. Commun. 49 (12) (2013) 1223–1225, https://doi.org/10.1039/C2CC38366G.
[16] A.D. MacKerell, D. Bashford, M. Bellott, et al., All-atom empirical potential for molecular modeling and dynamics studies of proteins, J. Phys. Chem. B 102 (1998) 3586–3616, https://doi.org/10.1021/jp973084f.
[17] J.E. Jones, On the determination of molecular fields.—II. From the equation of state of a gas, Proc. Roy. Soc. Lond.: Mathematical, Physical and Engineering Sciences. The Royal Society 106 (738) (1924) 463–477, https://doi.org/10.1098/rspa.1924.0082.
[18] D.M. Eike, E.J. Maginn, Atomistic simulation of solid-liquid coexistence for molecular systems: application to triazole and benzene, J. Chem. Phys. 124 (2006) 164503, https://doi.org/10.1063/1.2188400.
[19] Y. Zhang, E.J. Maginn, A comparison of methods for melting point calculation using molecular dynamics simulations, J. Chem. Phys. 136 (2012) 317, https://doi.org/10.1063/1.3702587.
[20] S. Karaman, A. Karaipekli, A. Sarı, et al., Polyethylene glycol (PEG)/diatomite composite as a novel form-stable phase change material for thermal energy storage, Sol. Energy Mater. Sol. Cell. 95 (2011) 1647–1653, https://doi.org/10.1016/j.solmat.2011.01.022.
[21] S. Jayaraman, Computing Thermodynamic and Transport Properties of Room Temperature Ionic Liquids and Molten Salts from Atomistic Simulations, University of Notre Dame, 2010.
[22] I. Pasquali, L. Comi, F. Pucciarelli, et al., Swelling, melting point reduction and solubility of PEG 1500 in supercritical CO2, Int. J. Pharm. 356 (2008) 76–81, https://doi.org/10.1016/j.ijpharm.2007.12.048.
[23] M. Constantinescu, L. Dumitrache, D. Constantinescu, et al., Latent heat nano composite building materials, Eur. Polym. J. 46 (2010) 2247–2254, https://doi.org/10.1016/j.eurpolymj.2010.09.007.
[24] A. Henry, G. Chen, High thermal conductivity of single polyethylene chains using molecular dynamics simulations, Phys. Rev. Lett. 101 (2008) 235502, https://doi.org/10.1103/PhysRevLett.101.235502.
[25] D. Li, Y. Wu, P. Kim, et al., Thermal conductivity of individual silicon nanowires, Appl. Phys. Lett. 83 (2003) 2934–2936, https://doi.org/10.1063/1.1616981.
[26] T. Uemura, S. Horike, K. Kitagawa, et al., Conformation and molecular dynamics of single polystyrene chain confined in coordination nanospace, J. Am. Chem. Soc. 130 (2008) 6781–6788, https://doi.org/10.1021/ja800087s.
[27] S. Karaman, A. Karaipekli, A. Sarı, et al., Polyethylene glycol (PEG)/diatomite composite as a novel form-stable phase change material for thermal energy storage, Sol. Energy Mater. Sol. Cell. 95 (2011) 1647–1653, https://doi.org/10.1016/j.solmat.2011.01.022.